The Plant Cell, Vol. 4, 1237–1249, October 1992 © 1992 American Society of Plant Physiologists

Ovule Development in Wild-Type Arabidopsis and Two Female-Sterile Mutants

Kay Robinson-Beers,[a] Robert E. Pruitt,[b,1] and Charles S. Gasser [a,2]

[a] Department of Biochemistry and Biophysics, University of California, Davis, California 95616
[b] Department of Genetics and Cell Biology, University of Minnesota, St. Paul, Minnesota 55108

Ovules are complex structures that are present in all seed bearing plants and are contained within the carpels in flowering plants. Ovules are the site of megasporogenesis and megagametogenesis and, following fertilization, develop into seeds. We combined genetic methods with anatomical and morphological analyses to dissect ovule development. Here, we present a detailed description of the morphological development of Arabidopsis ovules and report on the isolation of two chemically induced mutants, *bell* (*bel1*) and *short integuments* (*sin1*), with altered ovule development. Phenotypic analyses indicated that *bel1* mutants initiate a single integument-like structure that develops aberrantly. *sin1* mutants initiate two integuments, but growth of the integuments is disrupted such that cell division continues without normal cell elongation. Both mutants can differentiate archesporial cells, but neither forms a normal embryo sac. Genetic analyses indicated that *bel1* segregates as a single recessive mutation, and complementation tests showed that the two mutants are not allelic. The phenotypes of the mutants indicate that normal morphological development of the integuments and proper embryo sac formation are interdependent or are governed in part by common pathways. The ovule mutants that we describe in Arabidopsis represent novel genetic tools for the study of this stage of reproductive development.

INTRODUCTION

Flowers are typically viewed as having four types of organs: sepals and petals (sterile organs) and stamens and carpels (fertile organs). Significant progress in understanding the genetic mechanisms that specify the identity of organs formed in each whorl has been made through analysis of mutants in this process (Bowman et al., 1991b; Coen and Meyerowitz, 1991). Following specification of organ identity, an additional set of complex structures, the ovules, develop within the carpels. The occurrence of normal ovules in floral organs that have undergone a homeotic conversion to carpel-like structures (Bowman et al., 1989) demonstrates that ovule development is controlled by determinants that are subordinate to, but distinct from, those involved in floral organ specification. Analysis of the control of ovule development has been hampered because few ovule mutants have been described, even among plant species that have been subject to extensive genetic analysis. For example, although numerous morphological mutants affecting flower and carpel development have been described in Arabidopsis (Koornneef et al., 1983; Bowman et al., 1989; Okada et al., 1989), a poorly penetrant mutation, *Gf*, that affects the female gametophyte (Rédei, 1965) remains the only example of a lesion in Arabidopsis ovule formation. Two mutants of tobacco, *Mgr3* and *Mgr9*, that produce style-like outgrowths from their ovule primordia have only recently been described (Evans and Malmberg, 1989).

Much is known about the structure of the angiosperm ovule and its role in sexual reproduction. An ovule is comprised of a nucellus (megasporangium), which consists of both vegetative and sporogenous cells; one or, most commonly, two integuments, which envelop the nucellus; and the funiculus, a stalk that attaches the ovule to the placenta (Esau, 1965). Each of these tissues or substructures is diploid and part of the sporophytic generation of the plant. Within the nucellus, a sporogenous cell undergoes meiosis (megasporogenesis), and the megagametophyte (embryo sac) is produced by the mitotic division of one or several of the haploid products. For Arabidopsis and most other monosporic species (those in which the embryo sac develops from a single haploid megaspore), the megaspore nucleus divides mitotically into eight nuclei. The nuclei are apportioned into six uninucleate cells—one of which is the egg cell—and a seventh, binucleate central cell, whose two nuclei subsequently fuse into a single diploid nucleus. Following fertilization of both the egg cell and the central cell, the embryo and endosperm develop, and the integuments undergo structural and biochemical specialization as the ovule becomes a seed.

Our knowledge of the evolutionary origin of ovules is incomplete. In contrast to sepals, petals, stamens, and carpels, which are believed to represent modified leaves (Arber, 1937), the derivation of the angiosperm ovule and its parts is unclear.

[1] Current address: Department of Cellular and Developmental Biology, Harvard University, Cambridge, MA 02138.
[2] To whom correspondence should be addressed.

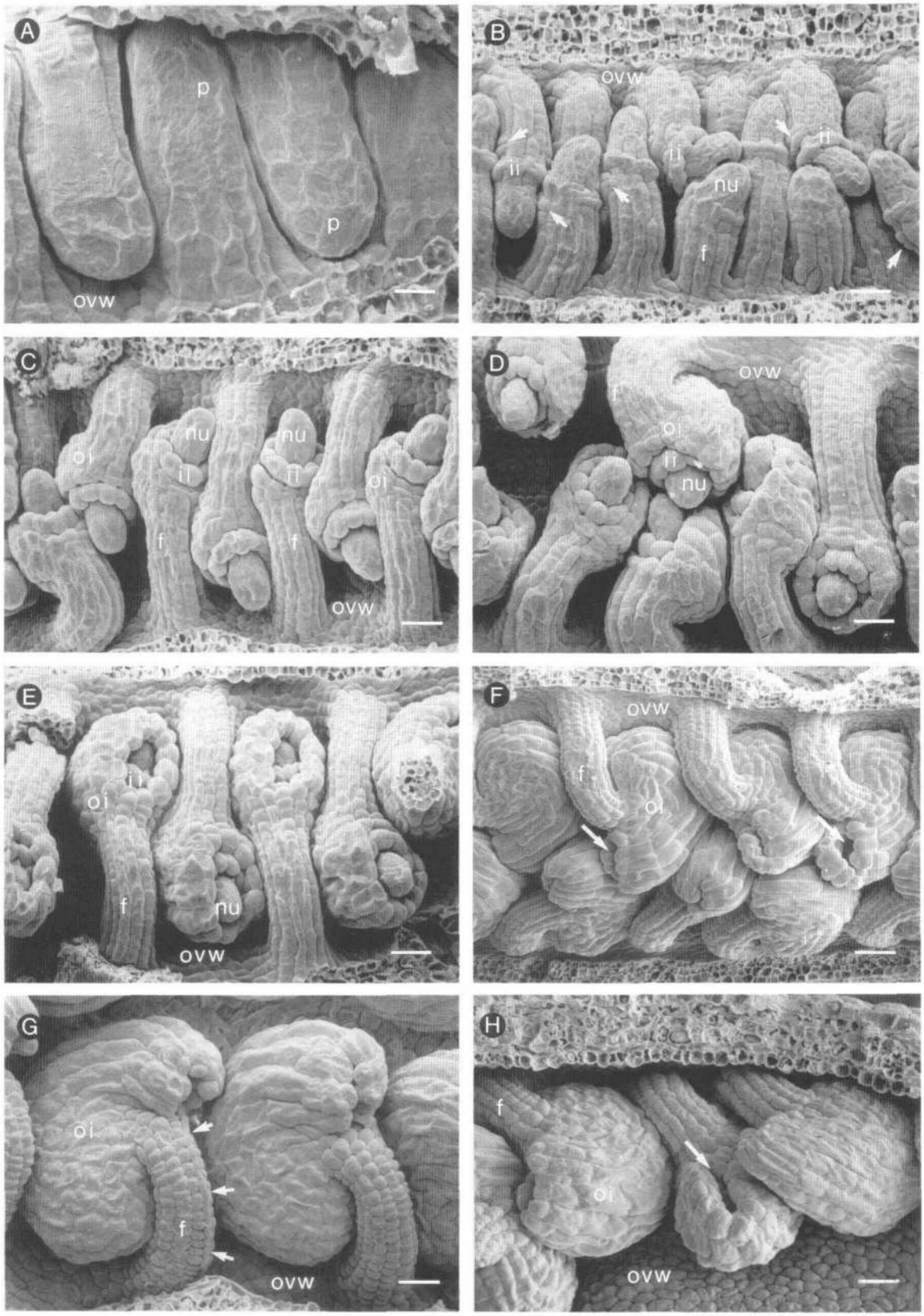

Figure 1. Ovule Development in Wild-Type Arabidopsis.

Whereas the ovule is often simply defined as an integumented megasporangium, neither the nucellus nor the integuments has a clear phyletic origin (Taylor, 1981; Gifford and Foster, 1989). To date, the best available evidence for the origin of the integuments comes from fossils of the extinct, Paleozoic seed ferns (Andrews, 1963). Among these plants exists a phylogenetic series that appears to indicate that the integument was formed through the fusion of sterile branches surrounding a megasporangium. However, paleobotanical evidence indicates that the inner and outer integuments of angiosperms are likely to have had separate origins (Doyle, 1978; Crane, 1985). The occurrence of the first ovules in the fossil record is contemporaneous with the first appearance of leaves, both of which occur long before the evolution of the angiosperm carpel (Taylor, 1981; Gifford and Foster, 1989). Thus, although ovules are contained within the carpels, their evolutionary origin indicates that ovules represent distinct structures. In addition, in terms of the phyletic origin of their parts and degree of histological differentiation, ovules are at least equal in complexity to archetypal floral organs such as sepals or petals. Taken together, these observations indicate that ovules could be viewed as additional floral organs.

To provide the necessary genetic tools for the study of ovule development, we have screened a mutagenized population for female-sterile mutants. In a subset of such mutants, sterility would be expected to result from defects in the function or formation of ovules. To date, two female-sterile mutants of Arabidopsis with morphologically abnormal ovules that also lack normal embryo sacs have been isolated. In this paper, we describe these mutants and contrast the morphological development of their ovules with that of wild-type ovules.

RESULTS

Wild-Type Ovule Development

Previous descriptions of ovule development in Arabidopsis have focused on megasporogenesis and megagametogenesis and have provided only brief reference to ovule morphology (Misra, 1962; Webb and Gunning, 1990; Mansfield and Briarty, 1991; Mansfield et al., 1991; Webb and Gunning, 1991). Because a more complete description of ovule formation facilitates the interpretation of ovule mutants, we undertook such a characterization using scanning electron microscopy. Our observations are illustrated in Figure 1, and in Table 1 are referenced to stages in overall floral development as described by Smyth et al. (1990).

In Arabidopsis, ovule primordia arise from the inner ovary wall in stage 9 and elongate and become finger-like during stage 10 (Figure 1A). The inner integument is initiated at the onset of stage 11 through a series of cell divisions in the L1 or dermal layer at a short distance behind the apex (Figure 1B). The divisions spread circumferentially and form a ring-like welt that delimits the nucellus as the apical portion of the primordium. At the end of stage 11, the outer integument is initiated behind the inner integument through a series of similar cell divisions (Figure 1B).

Extensive growth and development occur throughout stage 12 (Figures 1C to 1F). In early stage 12, as the body of the ovule enlarges and the funiculus elongates, the ovule begins to exhibit the effects of asymmetric growth that will produce the final amphitropous configuration. The developing ovule becomes S-shaped: near its attachment to the placenta, the funiculus bends backward and near its attachment to the nucellus and integuments (referred to as the chalaza), the funiculus bends forward (Figure 1C). Consequently, the long axis of the nucellus becomes perpendicular to the funiculus (Figure 1D). In addition, shortly after initiation, the outer integument takes on a wedge- and then cap-shaped appearance in early stage 12 (Figures 1C and 1D). The larger number of cells on the convex side, relative to the concave side, indicate that this morphology results from a greater number of cell divisions on the convex side. Subsequently, the integuments grow upward and keep pace with the enlargement of the nucellus. During this process, both the nucellus and integuments curve forward. During late stage 12, the outer integument overtakes the inner integument (Figure 1E), such that it begins to cover the latter as well as the nucellus. Both integuments envelop the

Figure 1. (continued).

Structures are given the following abbreviations: f, funiculus; ii, inner integument; nu, nucellus; oi, outer integument; ovw, ovary wall; p, ovule primordium.
(A) Elongate ovule primordia from a stage 10 flower. Bar = 5 μm.
(B) Ovule primordia from a stage 11 flower with newly initiated inner and outer integuments. Arrows point to outer integument. Bar = 19 μm.
(C) Ovules from an early stage 12 flower. The funiculus curves backward near its base and forward near the nucellus and the insertion of the integuments. The outer integument has become wedge- or cap-shaped. Bar = 19 μm.
(D) Ovules from a mid stage 12 flower. The integuments grow upward as the nucellus enlarges and curves forward. The long axis of the nucellus has become perpendicular to the funiculus. Bar = 19 μm.
(E) Ovules from a late stage 12 flower. The outer integument has covered both the inner integument and the nucellus. Bar = 19 μm.
(F) Ovules from a stage 13 flower. Both integuments completely envelop the nucellus, and the micropyle appears as a small cleft surrounded by markedly elongated cells of the outer integument. Arrows point to the micropyle. Bar = 29 μm.
(G) and **(H)** Lateral **(G)** and micropylar **(H)** views of ovules from flowers at stage 14. The micropyle is positioned near the funiculus. Arrows indicate a pollen tube on the surface of the funiculus in **(G)**. Arrow indicates micropyle in **(H)**. Bars = 17 μm.

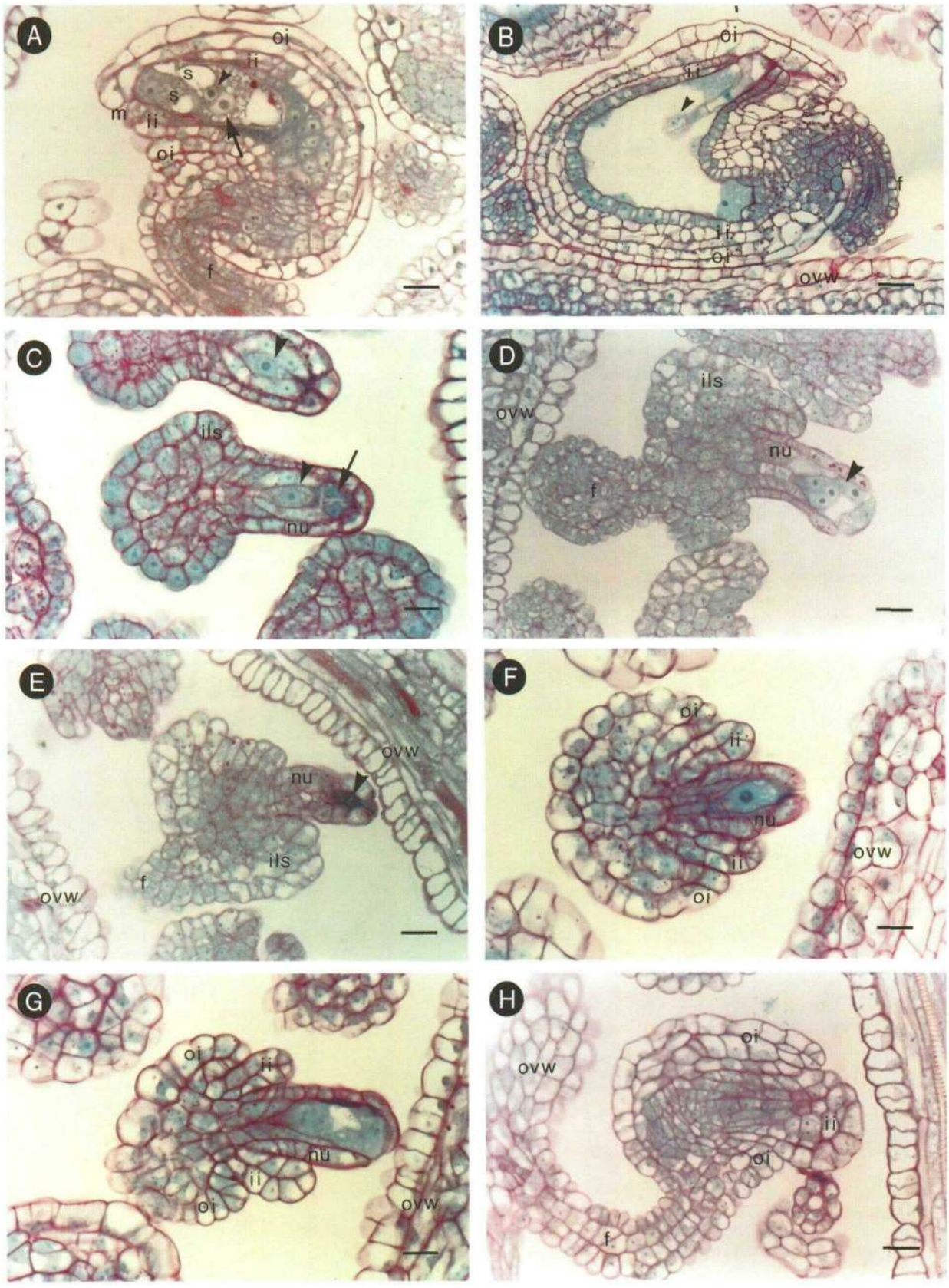

Figure 2. Light Micrographs of Developing Wild-Type and Mutant Ovules.

Table 1. Summary of Stages in Wild-Type and Mutant Ovule Development

Stage	Floral Landmark[a]	Wild Type	*bel1*	*sin1*
9	Petals stalked at base; gynoecial cylinder constricted at top	Ovule primordia arise	As in w. t.[b]	As in w. t.
10	Petals level with short stamens; gynoecial cylinder closed at top	Ovule primordia elongate	As in w. t.	As in w. t.
11	Stigmatic papillae appear	Inner and outer integuments initiated; megasporogenesis occurs	Single integument-like structure (ILS) initiated	As in w. t.
12 Early	Petals level with long stamens	Funiculus and nucellus curve; outer integument exhibits asymmetric growth; megagametogenesis initiated	Funiculus and nucellus curve; ILS exhibits asymmetric growth	As in w. t.
12 Mid		Integuments grow upward around nucellus	ILS expands but does not grow upward	As in w. t.
12 Late		Outer integument begins to cover both inner integument and nucellus; megagametogenesis complete	ILS enlarges into a collar of tissue; protuberances may develop	Cell division continues in integument; cell elongation retarded
13	Buds open; anthesis	Integuments envelop nucellus; micropyle positioned near funiculus	ILS continues to enlarge	As above
14	Long stamens extend above stigma	Fertilization occurs; embryo sac becomes increasingly curved	Development arrested	Development arrested

[a] Event marking beginning of stage as described (Smyth et al., 1990; Bowman et al., 1991a).
[b] w. t., wild type.

nucellus by the onset of stage 13, and the micropyle (a small opening in the integuments through which the pollen tube usually enters) appears as a small cleft surrounded by markedly elongated cells of the outer integument (Figure 1F). Figures 1G and 1H illustrate the morphology of the ovule at the time of fertilization (stage 14). The micropyle is positioned near the insertion of the funiculus, and the curvature of the funiculus closely follows the back of the outer integument (Figure 1G).

Figure 2 illustrates the internal organization of ovules characterized through the examination of serial sections of plastic embedded tissue. At anthesis (stage 13), the embryo sac of wild-type ovules is fully formed and consists of seven cells:

Figure 2. (continued).

Ovule structures are given the following abbreviations: f, funiculus; ii, inner integument; ils, integument-like structure; oi, outer integument; m, micropyle; nu, nucellus; ovw, ovary wall; s, synergid.

(A) Ovule from a wild-type flower at stage 13 with fully formed embryo sac. Arrowhead indicates the egg cell in contact with the two synergids. Large arrow indicates the secondary nucleus of the central cell. Antipodals are not visible in this section. Bar = 16 μm.

(B) Ovule from a wild-type flower at stage 15. Embryo sac has become highly curved following fertilization. Arrowhead indicates quadrant embryo. Bar = 25 μm.

(C) Developing ovule of *bel1* mutant from stage 11 flower with multiplanar tetrad. Arrow indicates three densely staining cells of the tetrad that are degenerating; arrowheads indicate surviving cells that are enlarging. Bar = 10 μm.

(D) Ovule of *bel1* mutant from stage 13 flower. Arrowhead indicates aberrant "embryo sac" with five cells; a portion of the nucellar epidermis is absent. Bar = 16 μm.

(E) Ovule of *bel1* mutant from stage 13 flower. Arrowhead indicates degenerated "embryo sac." Bar = 16 μm.

(F) Developing ovule of *sin1* mutant from stage 11 flower with enlarged archesporial cell. Bar = 10 μm.

(G) Ovule of *sin1* mutant from a stage 12 flower. The binucleate cell (produced by the division of the archesporial cell nucleus) inside the nucellus is undergoing a second nuclear division. Bar = 10 μm.

(H) Section of ovule of *sin1* mutant from flower at stage 13. The plane of section is just outside of the nucellus. The number of cells visible in the outer integument is equivalent to the number in wild type (Figure 2A). Bar = 16 μm.

an egg cell closely associated with two synergids at the micropylar end of the embryo sac, a large central cell with a diploid secondary nucleus, and three ephemeral antipodal cells located opposite the micropyle at the chalazal end of the embryo sac (Figure 2A). Most of the embryo sac lies in direct contact with the inner integument, the nucellar cells lying closest to the micropyle having degenerated during embryo sac formation. The integuments consist of well-defined, parallel cell layers. Shortly after fertilization (stage 15), the embryo sac has enlarged greatly and become highly curved so as to be nearly horseshoe-shaped (Figure 2B). This additional curvature is diagnostic of the amphitropous ovule. The innermost layer of the inner integument stains intensely, indicating the differentiation of a tissue referred to as the integumentary tapetum or endothelium (Kapil and Tiwari, 1978; Bowman et al., 1991a).

Isolation of the *bel1* and *sin1* Mutants

A screen for female-sterile plants was conducted on an M_2 population derived from ethyl methanesulphonate (EMS)-mutagenized seed of the Landsberg *erecta* ecotype. Plants were initially scored for general infertility by selecting those plants whose siliques completely failed to expand. A subset of these plants was determined to be female sterile through reciprocal backcrosses to wild-type plants. Only plants that are bona fide female steriles will fail to set any seed following pollination with wild-type pollen, but will successfully pollinate and fertilize wild-type pistils. Of approximately 25,000 M_2 plants screened, two female-sterile mutants were isolated. Cursory examination of dissected pistils from the mutant plants showed the ovules of both mutants to be morphologically abnormal. Further study (see below) led us to designate the two mutants *bell* (*bel1*), after its bell-shaped ovules, and *short integuments* (*sin1*).

Gross Phenotypic Analysis of Mutants

Figure 3 shows that the *bel1* mutant exhibits an overall appearance that is similar to that of a wild-type plant. The data in Table 2 show that leaf size and internode length of *bel1* mutants do not differ significantly from wild type. The only appreciable differences between the vegetative morphology of wild-type and *bel1* plants result from the infertility of the mutants. As a result of the *bel1* mutant's failure to set seed, senescence is delayed and development of axillary buds continues, leading to a highly branched inflorescence (Figure 3, cf. left and center plants). This same growth habit occurs in other infertile Arabidopsis mutants (Feldmann, 1991). Gross floral morphology of *bel1* mutants is indistinguishable from that of wild-type plants, and only unexpanded siliques and abnormal ovule morphology distinguish *bel1* mutants from wild-type plants.

The *sin1* mutant exhibits pleiotropic effects. Although the rosette morphology is roughly equivalent to that of wild-type plants (Figure 3, cf. left and right plants), leaves are measurably smaller and internode lengths are shorter in the inflorescence (Table 2). The pronounced shortening of internodes between successive flowers gives the inflorescence a compacted appearance (Figure 3, right plant). The first formed flowers of *sin1* mutants are completely infertile and somewhat morphologically juvenile. Late formed flowers are morphologically normal and, although male fertile, produce visibly less pollen than wild-type flowers.

Figure 3. Wild-Type Arabidopsis (left) and Representative *bel1* (center) and *sin1* (right) Mutants.

All plants in populations segregating for either the *bel1* or *sin1* mutation exhibit either clear wild-type or mutant phenotypes and all wild-type heterozygous plants set normal numbers of seed, indicating that these mutations are neither megagametophytic nor embryo lethal.

Ovule Development in *bel1* Mutants

Figure 4 illustrates important stages in the development of *bel1* ovules, which are compared to stages of development of wild-type ovules in Table 1. Through stage 10, development of *bel1* ovules is similar to that of wild-type ovules (cf. Figures 1A and

4A). However, in stage 11, only a single integument-like structure is initiated at the base of the nucellus (Figure 4B). Furthermore, from its initiation, the structure is relatively wide and is comprised of several rows of cells, resembling in appearance the outer integument of wild-type ovules (in wild-type ovules, the inner integument is initiated first, is narrower, and is comprised of fewer cells; cf. Figures 1B and 4B). Through early stage 12, the single integument-like structure continues to resemble the outer integument of wild-type ovules by developing a wedge- and then cap-shaped appearance as a result of asymmetric growth (cf. Figures 1C and 4C). As is the case with wild-type ovules, *bel1* ovules become S-shaped, appearing to bend backward near the placenta and forward near the insertion of the integument-like structure (Figures 4C and 4D). Similarly, the long axis of the nucellus of a *bel1* ovule gradually becomes perpendicular to the funiculus (Figures 4E and 4F).

By late stage 12, the integument-like structure becomes enlarged and thickened, ceases to resemble the outer integument of wild-type ovules, and appears quite abnormal (Figures 4D and 4E). It fails to grow upward and develop the shape of the wild-type outer integument and instead becomes a thick collar of tissue that never envelops the nucellus. In addition, in approximately 25% of *bel1* ovules, the integument-like structure exhibits protuberances (Figure 4F). The protuberances vary in number from zero to four, with three being the most common number. At stage 14, ovules of *bel1* mutants are bell-shaped, have exposed nucelli, and lack normal integuments (Figure 4G). Occasionally, additional protuberances occur at the base of the nucellus, interior to the outer integumentary structure (Figure 4H). In addition to the aberrant expansion of the integument-like structures, the funiculi of *bel1* ovules are thicker and consist of more cells than wild-type funiculi (cf. Figures 1G and 1H and Figures 4G and 4H). Whereas integuments in wild-type ovules are organized into well-defined layers of elongated cells (Figure 2A), sections through stage 14 *bel1* ovules (Figures 2D and 2E) reveal no similar layered organization in the integument-like structure. The internal organization of the integument-like structure, therefore, differs significantly from either integument of wild-type ovules.

Table 2. Morphometric Comparisons between Ovule Mutants and Wild-Type Plants

Variety	Longest Leaves (mm)[a,b]	First Internode of Inflorescence	Nodes between Flowers[c]
Wild type	24.7 ± 3.0	45.6 ± 12.1	8.6 ± 2.9
sin1	18.8 ± 3.0[d]	30.2 ± 7.8	1.4 ± 1.0[d]
bel1	20.0 ± 3.7	40.6 ± 22	8.4 ± 3.3

[a] All measurements were performed on seven wild-type, nine *sin1*, and 24 *bel1* plants.

[b] The three longest leaves were measured on each plant.

[c] The length of the first six nodes between flowers was measured on the primary inflorescence of each plant.

[d] Significantly different from wild type ($P < 0.01$).

Ovules of *bel1* mutants fail to produce normal embryo sacs. Anatomical examination of early stages revealed that a small subset of *bel1* ovules fails to differentiate archesporial cells (data not shown). In other ovules, archesporial cells differentiate and divide to form tetrahedral or decussate tetrads (Figure 2C), which closely resemble the megaspores produced by meiosis in normal ovules (termed multiplanar tetrads by Webb and Gunning, 1990). The members of the tetrad nearest the micropyle degenerate (Figure 2C). The surviving cell undergoes several subsequent divisions (Figure 2D). These divisions result in a maximum of five cells that do not resemble the normal seven-celled, eight-nucleate embryo sac of wild-type ovules (Figure 2D). In some cases, these cells are exposed by the degeneration of the nucellar epidermis that occurs at, or just prior to, anthesis, with subsequent degeneration of the cells (Figure 2E). Thus, at anthesis (stage 13), siliques contain both ovules with undifferentiated nucelli and ovules whose nucelli contain either an abnormal "embryo sac" composed of a group of several enlarged cells or degenerated cellular material in the same location.

Ovule Development in *sin1* Mutants

Figures 5A and 5B show that through stage 11 ovules of the *sin1* mutant resemble wild-type ovules. Both inner and outer integuments are initiated in stage 11 (Figure 5B). Through mid stage 12, ovules of *sin1* mutants continue to resemble wild-type ovules, including proliferation of cells of the integument and curvature of the funiculus and nucellus (cf. Figures 1D and 5C). However, by the time of fertilization (stage 14), although the two integuments of the *sin1* mutant ovules have enlarged, they still have not covered the nucellus (Figure 5D). Whereas the ovules of the *sin1* mutant at anthesis are morphologically similar to wild-type and *sin1* ovules at stage 11, they are roughly twice as large, and the outer integument can be seen to consist of many more cells (Figures 5A, 5B, and 5D). In fact, the number of cells in the outer integument often approximates that in the outer integument of wild-type ovules (cf. Figures 2A and 2H). As seen in wild-type ovules, and in contrast to ovules of *bel1* mutants, the cells of the integuments are organized into distinct cell layers (Figure 2H). Thus, in *sin1* mutants, cell division continues in the integuments after stage 11, but this division is not accompanied by the directional cell expansions that are necessary for normal ovule morphology.

We also examined the ovules of flowers at stages 16 and 17 to ascertain whether morphological development is simply delayed rather than disrupted. Ovules from the later stage flowers appear similar to those in stage 14 and degenerate without further morphological development (data not shown). Stages in *sin1* ovule development are compared to those of wild type in Table 1.

Ovules of *sin1* mutants also fail to form normal embryo sacs. Anatomical analyses of developing *sin1* ovules indicated that whereas some ovules remain undifferentiated, most ovules differentiate an archesporial cell. Subsequently, the

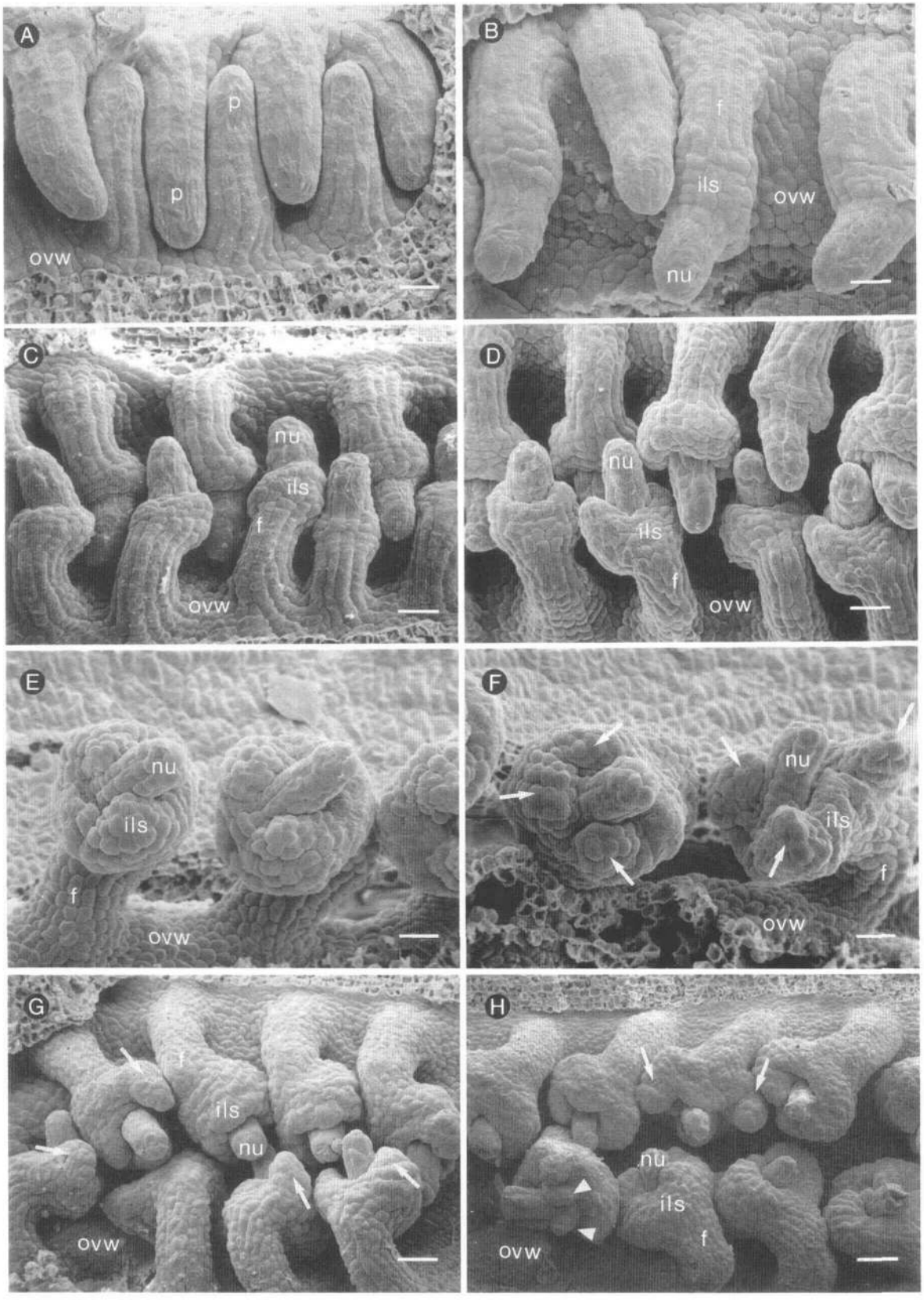

Figure 4. Ovule Development in *bel1* Mutants.

archesporial cell undergoes nuclear divisions without cytokinesis to produce a binucleate cell (Figure 2F). An additional nuclear division is also occasionally observed (Figure 2G). The product of these divisions then degenerates at or shortly after anthesis (Figure 2H). Thus, we observed neither the complete formation of a tetrad of megaspores nor the formation of a normal embryo sac.

Genetic Analyses

The heritability of the mutant phenotypes of both *bel1* and *sin1* has been confirmed by three subsequent backcrosses to wild-type plants. All F_1 progeny from such crosses had wild-type phenotypes. Data on the phenotypes of the F_2 progeny are presented in Table 3. Segregation ratios of approximately 3:1 and 3.7:1 (wild type:mutant) were observed for the *bel1* and *sin1* mutants, respectively. Statistical analysis indicated that the segregation of the *bel1* mutant is consistent with it being a single recessive mutation (Table 3). Similar analysis of the *sin1* mutant showed that we cannot reject the hypothesis that it arises from a single gene recessive mutation, but we can reject the possibility that it results from two unlinked loci (Table 3).

A complementation test was performed to determine whether these mutations were allelic. Mutant plants were used as pollen parents in crosses with wild-type plants to create known heterozygotes. The F_1 heterozygotes of the two mutants were then crossed to each other, and all of the resulting progeny had wild-type phenotypes, indicating that the two were nonallelic. As a further test and to rule out the possibility of a lethal *sin1/bel1* heterozygote, all of the plants were allowed to self-pollinate, and a sample of the seed from each plant was sown as a family. Several of these families segregated for both *sin1* and *bel1*, and double mutants were isolated from such families. Taken together, these data indicated that *sin1* and *bel1* define two separate loci for genes that we designate *SIN1* and *BEL1*.

bel1, *sin1* double mutants exhibit a largely additive phenotype. As is the case for ovules of *bel1* mutants, only a single integument-like structure is initiated, and some ovules have protuberances located at the periphery of the structure (Figures 5E and 5F). However, as is the case for ovules of *sin1* mutants, expansion of the integument-like structure is limited relative to that seen in *bel1* mutants. At anthesis, the ovules have exposed nucelli, whose curvature is readily apparent, and exhibit a thickening of the funiculus that is similar to that observed in *bel1* ovules (Figure 5F).

Table 3. Segregation of Ovule Mutants

	Wild Type:Mutant		
Mutant	Observed	Expected	χ^2
sin1	235:63 (3.7:1)	3:1[a]	2.16, $P > 0.10$
		15:1[b]	106.4, $P << 0.001$
bel1	255:86 (3.0:1)	3:1[a]	0.001, $P > 0.95$

[a] Single locus recessive mutation.
[b] Mutant phenotype resulting from two unlinked loci.

DISCUSSION

To establish a basis for the phenotypic analysis of ovule mutants, we provide a detailed description of the morphological development of wild-type Arabidopsis ovules. In combination with recently published descriptions of megasporogenesis (Webb and Gunning, 1990), megagametogenesis (Mansfield et al., 1991), and early embryogenesis (Mansfield and Briarty, 1991; Webb and Gunning, 1991), our study completes a portrait of one portion of the Arabidopsis life cycle. Earlier studies of ovules of the Brassicaceae described the histological origin of both the ovule primordium and the integuments. Bouman (1984) has reported that ovules of the Brassicaceae arise from three cell layers (the dermal, subdermal, and third cell layer designated L1, L2, and L3) of the placenta. Roth (1957) detailed the histogenesis of the integuments of *Capsella bursa-pastoris* and reported that both the inner and the outer integument arise from the L1 or dermal layer.

Figure 4. (continued).

Structures are given the following abbreviations: f, funiculus; ils, integument-like structure; nu, nucellus; ovw, ovary wall; p, ovule primordium.
(A) Elongate ovule primordia from a flower at stage 10. Bar = 11 μm.
(B) Ovule primordia from a flower at stage 11 with single integument-like structure. Bar = 11 μm.
(C) Ovules from a flower at early stage 12. Integument-like structure has developed a wedge-shaped appearance as a result of asymmetric growth. Bar = 19 μm.
(D) Ovules from a flower at mid stage 12. Although the nucellus and funiculus curve as in wild-type ovules, the integument-like structure fails to grow upward. Bar = 19 μm.
(E) and **(F)** Ovules from flowers at late stage 12. The integument-like structure has failed to cover the nucellus and has become a thick collar of tissue. Arrows in **(F)** point to protuberances of the integument-like structure. Bar = 18 μm.
(G) and **(H)** Ovules from flowers at stage 14. At the time of fertilization, *bel1* ovules are bell-shaped and have exposed nucelli and a single abnormal integument-like structure. Arrows point to protuberances of the integument-like structure. Arrowheads in **(H)** indicate rare additional protuberances that develop at the base of the nucellus. Bar = 26 μm.

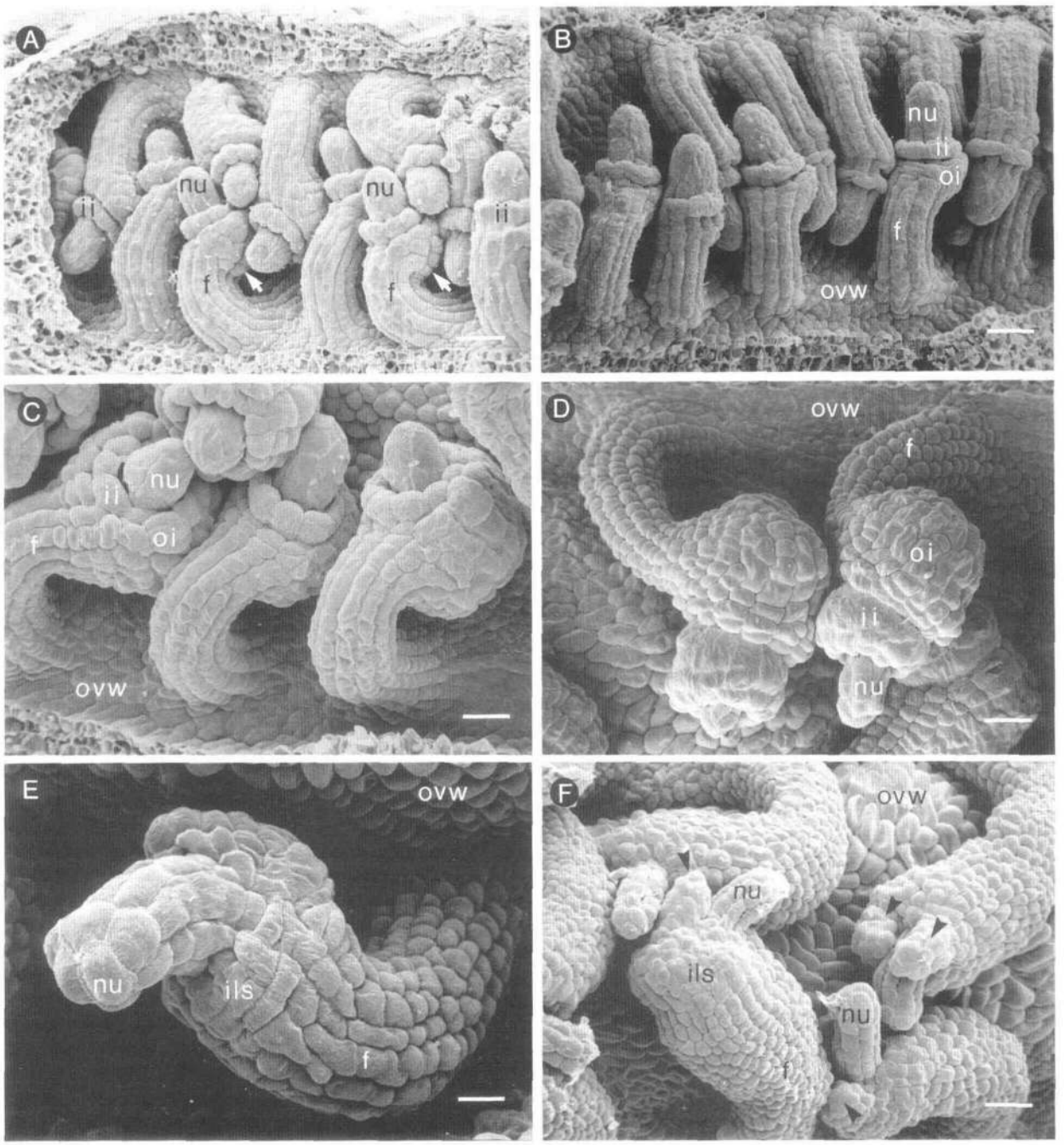

Figure 5. Ovule Development in *sin1* Mutants and Phenotype of the *sin1*, *bel1* Double Mutant.

Structures are given the following abbreviations: f, funiculus; *ii*, *inner integument*; *ils*, *integument-like* structure; nu, nucellus; oi, outer integument; ovw, ovary wall.

(A) and **(B)** Wild-type ovules **(A)** and *sin1* ovules **(B)** from flowers at early stage 12. During early development *sin1* ovules resemble wild-type ovules. Arrows in **(A)** point to outer integument. Bars = 19 μm.

(C) Ovules of *sin1* mutants from flowers at mid stage 12. *sin1* ovules continue to resemble wild-type ovules (cf. Figure 1D). Bar = 13 μm.

(D) Ovules of *sin1* mutants from flowers at stage 14. Although the ovules are morphologically similar to ovules in stage 11, they have doubled in size, and their integuments consist of many more cells. In addition, the nucellus remains uncovered. Bar = 17 μm.

(E) and **(F)** Ovules of *sin1*, *bel1* double mutants from flowers at stage 13. Only a single integument-like structure is formed and its growth is limited. *The nucelli remain* exposed and the funiculi are thickened. Arrowheads in **(F)** indicate protuberances at the periphery of their integument-like structures. Bar in **(E)** = 8 μm; bar in **(F)** = 21 μm.

With respect to their final morphology, ovules are classified according to the shape and position of their parts. In an effort to ascertain phylogenetic significance, a minimum of three principal morphological types have been recognized: orthotropous, erect ovules in which the funiculus, nucellus, and micropyle all lie in a straight line; anatropous, the most common type among angiosperms, in which the micropyle is adjacent to the funiculus as a result of a 180° curvature of the funiculus; and campylotropous, in which the funiculus appears to be attached midway between the micropyle and the chalaza, as a result of curvature of the nucellus in addition to limited curvature of the funiculus (Gifford and Foster, 1989). Campylotropous ovules are unique in having curved embryo sacs; however, in the case in which the curvature is extreme, they are often classified as a fourth type, amphitropous (Bocquet, 1959).

We interpret ovules of Arabidopsis to be amphitropous. Although the micropyle of an Arabidopsis ovule lies adjacent to the funiculus, this position results primarily from forward curvature of the nucellus (Figure 2A). Ovules of Arabidopsis are transiently campylotropous at anthesis (Figure 2A). Following fertilization, however, the embryo sac becomes increasingly curved (Figure 2B), resulting in the final amphitropous configuration of the ovule. Our designation represents a refinement over that of others who have referred to Arabidopsis ovules as anatropous (Misra, 1962; Webb and Gunning, 1990; Mansfield et al., 1991) and is consistent with descriptions of ovules of four other genera in the Brassicaceae (*Cardamine*, *Draba*, and *Sisymbrium* [Vandendries, 1909] and *Capsella* [Roth, 1957]).

We have identified two female-sterile mutants of Arabidopsis, *bel1* and *sin1*, which have ovules with morphologically abnormal integuments. In addition, the ovules of each of these mutants fail to form normal embryo sacs. The two mutants do not complement one another and, therefore, define two separate loci. *bel1* segregates as a single gene recessive, and *sin1* most likely also represents a single gene recessive mutation (Table 3). Thus, mutations at two separate loci affect the development of the integuments as well as the female gametophyte, indicating that some genes required for normal integument development are also required for normal megagametogenesis. Although this observation does not in itself imply causality, it does indicate the possibility that embryo sac formation and integument development are interdependent or are governed in part by common pathways. As additional ovule mutants are identified in more extensive screens, it will be interesting to determine whether mutants with malformed integuments and normal embryo sacs, or the converse, can be isolated.

bel1 mutants produce ovules that initiate only a single integument that develops into an aberrant structure. In its early development, this structure does not resemble the first-formed, inner integument of wild-type ovules. Instead, it more closely resembles the development of the outer integument of wild-type ovules. Although at present we lack molecular markers for the inner and outer integument, based on the morphological data at hand we hypothesize that the inner integument is missing from the ovules of *bel1* mutants. In addition, although early development of the outer integument appears normal, its later development is aberrant. This implies a commonality of pathway between the initiation of the inner integument and the proper development of the outer integument.

The single integument-like structure of the *bel1* mutant is converted to a collar-like structure that may include a variable number of protuberances. It is interesting to note that two recently identified mutants of tobacco produce style-like outgrowths from ovule primordia (Evans and Malmberg, 1989). Although analyses of the tobacco mutants did not determine the specific portion of the ovule primordia from which the style-like structures develop, this observation indicates that some portion of an ovule primordium can be converted to a carpel-like structure. Thus, it is possible that the structures observed in *bel1* mutants represent partial conversion of the integument into other plant organs or organ primordia. Although this is an interesting speculation, to ascertain the nature of the *bel1* mutant's integument-like structure we will need to isolate and analyze additional alleles that vary in their degree of modification.

sin1 mutants produce ovules in which morphological development appears to stop, yet development as a whole is not arrested. Cell division in the integuments progresses without producing a normal structure. Initial study indicates that the number and arrangement of the cells of the outer integument are similar at anthesis for both *sin1* and wild-type ovules (cf. Figures 2A and 2H, 17 cells are visible in both). The morphological difference between the two appears to be due largely to a lack of proper cell enlargement in *sin1* ovules during stage 12. This result is not entirely surprising given the fact that elongation is apparently suppressed elsewhere in *sin1* mutants: internodes in the inflorescence are shorter than those in the inflorescences of wild-type plants (Table 2). Interestingly, however, the continued cell division without appropriate enlargement in the formation of the integuments indicates that the pathways for the control of cell division and cell enlargement may be separable in this structure.

Whereas we cannot exclude the possibility that the *sin1* mutation segregates as a single gene recessive, it appears that the frequency of obtaining *sin1* mutants is aberrantly low (Table 3). Nevertheless, the frequency is not so low as to be consistent with the segregation of two unlinked or weakly linked genes. Given the fact that the *sin1* mutation affects male fertility in homozygotes, in the haploid state it might also affect the vigor of the male gametophyte, resulting in a reduced frequency of *sin1* homozygous progeny.

Our study indicates that it may indeed be possible to dissect ovule development and megagametogenesis by using a combined genetic and structural approach similar to that which has been applied to investigations of control of floral organ identity (Bowman et al., 1991b; Coen and Meyerowitz, 1991). The mutants we have isolated represent a new class of morphological mutants of Arabidopsis and result from distinct defects in developmental programs occurring after floral organ specification has occurred. Our long range goal is to

identify and characterize all loci required for normal ovule development and to examine the genetic interactions among these loci. It is interesting to note that several genes with homology to the organ identity "MADS box" genes are expressed preferentially in ovules (Ma et al., 1991). These putative transcription factors are likely candidates for genes that will control aspects of ovule development. Determination of the relationships between these genes and those identified in our mutant studies will further aid in elucidation of factors controlling ovule development.

METHODS

Plant Material

Seeds were sown in a 1:1:1 mixture of perlite, fine vermiculite, and peat moss. Plants were grown under continuous fluorescent and incandescent illumination at 25°C and fertilized weekly with a complete nutrient solution (Kranz and Kirchheim, 1987). Genetic crosses were performed as previously described (Kranz and Kirchheim, 1987).

Mutant Isolation

Mutants were isolated from a screen of M_2 plants derived from ethyl methanesulphonate (EMS)-mutagenized seed of *Arabidopsis thaliana*, ecotype Landsberg *erecta*. Approximately 120,000 seeds were imbibed for 8 hr in the presence of 40 mM EMS and then washed for 18 hr in water. The seed was then sown in groups of approximately 500 M_1 plants. After the M_1 plants had set seed, the seed from each group was pooled by harvesting in bulk. For screening, approximately 500 seeds from each pool were planted. The M_2 plants were grown to maturity and screened for sterility by identifying those plants whose siliques failed to elongate. Sterile plants were tested for female sterility by pollination with wild-type pollen. Plants that were not rescued by this test were further tested for male fertility by backcrossing to a male-sterile line that does not form pollen. A total of 25,000 M_2 plants were screened and two female-sterile mutants whose flowers exhibit normal gross morphology were isolated. The F_1 plants resulting from the cross to a male-sterile line were grown, selfed, and checked for segregation. Individuals exhibiting the mutant phenotype were reselected and backcrossed to wild-type plants three times.

Light Microscopy

Pistils were quickly removed from flowers and further dissected to facilitate penetration of the fixative. Following dissection, pistils were immersed in 3% glutaraldehyde in cacodylate buffer (50 mM sodium cacodylate, pH 7.0) and placed under gentle vacuum (~100 torr). Following 2 to 4 hr of fixation at room temperature or overnight fixation at 4°C, specimens were rinsed four times in cacodylate buffer. Dehydration was carried out in a graded ethanol series, and specimens were infiltrated in mixtures of ethanol and Historesin (Cambridge Instruments, Deerfield, IL) over a period of 24 hr. Specimens were further infiltrated in pure Historesin for several days and then embedded in fresh Historesin. Polymerization was carried out at room temperature for 1 day.

Sections (3 to 4 μm) were cut with a Sorvall (part of DuPont Co., Newton, CT), Porter-Blum MT2 ultramicrotome using glass knives, transferred to drops of water on acid-washed slides, and dried overnight on a slide warming tray at 45°C. The sections were then stained with periodic acid and Schiff's reagent (O'Brien and McCully, 1981) followed by counterstaining with Aniline Blue Black (Fischer, 1968) and mounted in immersion oil. Sections were photographed on a Zeiss (Oberkochen, Germany) Axioplan microscope using bright-field illumination.

Scanning Electron Microscopy

Pistils were partially dissected and initially fixed in the same solution that was used to prepare specimens for light microscopy. Following slow release of the vacuum, specimens were stored in the same solution at 4°C. No specimen was stored for longer than 3 days. The fixed specimens were rinsed four times in cacodylate buffer and post-fixed in 2% Osmium tetroxide in cacodylate buffer overnight at 4°C. Specimens were again rinsed four times in cacodylate buffer and dehydrated in a graded series of ethanol. Critical point drying was carried out in liquid carbon dioxide. Specimens were mounted on stubs, dissected further, sputter coated with gold, and examined with an ISI DS130 scanning electron microscope at an accelerating voltage of 10 kV.

ACKNOWLEDGMENTS

We thank Michael Dunlap of the University of California, Davis, Facility for Advanced Instrumentation, and Catherine M. Geil for technical assistance; Professors Judy Callis, James A. Doyle, Ernest M. Gifford, Donald R. Kaplan, and Animesh Ray for helpful discussions; and Dr. Eric P. Beers for a critical reading of the manuscript. This work was supported by National Science Foundation Postdoctoral Fellowship in Plant Biology No. DCB 9008357 (to K.R.-B.) and by U.S. Department of Agriculture Grant No. 92-37304-7756, National Science Foundation Grant No. DCB 90-58284, and a grant from the Monsanto Company (to C.S.G.).

Received July 31, 1992; accepted August 25, 1992.

REFERENCES

Andrews, H.N.J. (1963). Early seed plants. Science **142,** 925–931.

Arber, A. (1937). The interpretation of the flower: A study of some aspects of morphological thought. Biol. Rev. **12,** 157–184.

Bocquet, G. (1959). The Campylotropous ovule. Phytomorphology **9,** 222–227.

Bouman, F. (1984). The ovule. In Embryology of the Angiosperms, B.M. Johri, ed (New York: Springer-Verlag), pp. 123–157.

Bowman, J.L., Smyth, D.R., and Meyerowitz, E.M. (1989). Genes directing flower development in *Arabidopsis*. Plant Cell **1,** 37–52.

Bowman, J.L., Drews, G.N., and Meyerowitz, E.M. (1991a). Expression of the Arabidopsis floral homeotic gene *AGAMOUS* is restricted to specific cell types late in flower development. Plant Cell **3,** 749–758.

Bowman, J.L., Smyth, D.R., and Meyerowitz, E.M. (1991b). Genetic interactions among floral homeotic genes of *Arabidopsis*. Development **112,** 1–20.

Coen, E.S., and Meyerowitz, E.M. (1991). The war of the whorls: Genetic interactions controlling flower development. Nature **353,** 31–37.

Crane, P.R. (1985). Phylogenetic analysis of seed plants and the origin of angiosperms. Ann. Mo. Bot. Gard. **72,** 716–793.

Doyle, J.A. (1978). Origin of the angiosperms. Ann. Rev. Ecol. Syst. **9,** 365–392.

Esau, K. (1965). Anatomy of Seed Plants (New York, NY: John Wiley and Sons).

Evans, P.T., and Malmberg, R.L. (1989). Alternative pathways of tobacco placental development: Time of commitment and analysis of a mutant. Dev. Biol. **136,** 273–283.

Feldmann, K.A. (1991). T-DNA insertion mutagenesis of *Arabidopsis*: Mutational spectrum. Plant J. **1,** 71–82.

Fischer, D.B. (1968). Protein staining of ribboned epon sections for light microscopy. Histochemie **16,** 92–96.

Gifford, E.M., and Foster, A.S. (1989). Morphology and Evolution of Vascular Plants (New York, NY: W.H. Freeman).

Kapil, R.N., and Tiwari, S.C. (1978). The integumentary tapetum. Bot. Rev. **44,** 457–490.

Koornneef, M., van Eden, J., Hanhart, C.J., Stam, P., Braaksma, F.J., and Feenstra, W.J. (1983). Linkage map of *Arabidopsis thaliana*. J. Hered. **74,** 265–272.

Kranz, A.R., and Kirchheim, B. (1987). *Arabidopsis* Information Service, Vol. 24: Genetic Resources in *Arabidopsis* (Frankfurt, Germany: Arabidopsis Information Service).

Ma, H., Yanofsky, M.F., and Meyerowitz, E.M. (1991). *AGL1-AGL6*, an *Arabidopsis* gene family with similarity to floral homeotic and transcription factor genes. Genes and Dev. **5,** 484–495.

Mansfield, S.G., and Briarty, L.G. (1991). Early embryogenesis in *Arabidopsis thaliana*. II. The developing embryo. Can. J. Bot. **69,** 461–476.

Mansfield, S.G., Briarty, L.G., and Erni, S. (1991). Early embryogenesis in *Arabidopsis thaliana*. I. The mature embryo sac. Can. J. Bot. **69,** 447–460.

Misra, R.C. (1962). Contribution to the embryology of *Arabidopsis thalianum* (Gay & Monn.). Univ. J. Res., Agra **11,** 191–198.

O'Brien, T.P., and McCully, M.E. (1981). The Study of Plant Structure: Principles and Methods (Melbourne: Termarcarphi Pty. Ltd.).

Okada, K., Komaki, M.K., and Shimura, Y. (1989). Mutational analysis of pistil structure and development of *Arabidopsis thaliana*. Cell Differ. Develop. **28,** 27–38.

Rédei, G. (1965). Non-mendelian megagametogenesis in *Arabidopsis*. Genetics **51,** 857–872.

Roth, I. (1957). Die Histogenese der Integumente von *Capsella bursa-pastoris* und ihre morphologische Deutung. Flora **145,** 212–235.

Smyth, D.R., Bowman, J.L., and Meyerowitz, E.M. (1990). Early flower development in *Arabidopsis*. Plant Cell **2,** 755–767.

Taylor, T.N. (1981). Paleobotany: An Introduction to Fossil Plant Biology (New York, NY: McGraw-Hill).

Vandendries, R. (1909). Contribution à l'histoire du développement des crucifères. La Cellule **25,** 413–459.

Webb, M.C., and Gunning, B.E.S. (1990). Embryo sac development in *Arabidopsis thaliana*.1. Megasporogenesis, including the microtubular cytoskeleton. Sex. Plant Reprod. **3,** 244–256.

Webb, M.C., and Gunning, B.E.S. (1991). The microtubular cytoskeleton during development of the zygote, proembryo and free-nuclear endosperm in *Arabidopsis thaliana* (L.) Heynh. Planta **184,** 187–195.